IEEE Access
Multidisciplinary | Rapid Review | Open Access Journal

Received 10 March 2023, accepted 22 March 2023, date of publication 5 April 2023, date of current version 17 April 2023.

Digital Object Identifier 10.1109/ACCESS.2023.3264568

RESEARCH ARTICLE

Three-Phase Dual-Winding Multitasked PMSM Machine Using Double Layer Concentrated Winding for HEV Application

TANVEER YAZDAN[1], MUHAMMAD HUMZA[2], AND HAN-WOOK CHO[2], (Member, IEEE)

[1]Department of Electrical Engineering, The University of Lahore, Lahore 54000, Pakistan
[2]Department of Electrical, Electronics, and Communication Engineering Education, Chungnam National University, Daejeon 34134, South Korea

Corresponding authors: Han-Wook Cho (hwcho@cnu.ac.kr) and Muhammad Humza (engr.humza7@gmail.com)

This work was supported by the National Research Foundation of Korea (NRF) Grant funded by the Korean Government under Grant 2022R1I1A3072104.

ABSTRACT This paper proposes a three-phase dual-winding permanent magnet synchronous machine (PMSM) providing multitasked operation for accessory drive systems in hybrid electric vehicles (HEV). The novelty of this research lies in the machine having special slots and pole combinations with specific configuration of two sets of double-layer concentrated group winding separated by the unwound tooth between the phase groups formed on the same stator to achieve both the motoring and generator operation simultaneously as well as independently. These operations are accomplished by incorporating motor and generator winding separately on the same stator of a single PMSM machine. This single machine is particularly designed to eliminate the mutual coupling between these two sets of windings such that the load variation on the generator does not affect the mechanical output power of the motor. To confirm this multitasking, the electromagnetic design of the machine has been presented, and its operating modes are analyzed. The performance is compared using finite element analysis with that of a conventional PMSM machine having a double-layer winding configuration.

INDEX TERMS Accessory drive system, double-layer concentrated winding, dual-winding machine, hybrid electric vehicles, permanent magnet synchronous machine.

I. INTRODUCTION

Hybrid electric vehicles (HEV) are a good candidate in the transport sector owing to better fuel economy and reduced greenhouse gas emissions [1], [2]. In conventional HEVs, the main power comes from two major sources of motion: the internal combustion engine (ICE) and electric motor which may be required to run accessory loads such as power steering, water pump, air conditioner, heating system, power windows, and lights, irrespective of the vehicle movement [3]. This power needs to be available on demand, which can be fulfilled by using either a drive-by-wire system or electric accessory drive (EAD) system in HEV. In the drive-by-wire technique, several electric motors of different power ratings, various inverters and their gate drive circuits, and a Lundell alternator are used to drive these accessory loads [3], [4]. This makes the system inefficient and increases the cost, and overall weight. Whereas an electrical accessory drive system delivers the power through a belt mechanism. In the EAD system, one motor and one generator convert energy into mechanical and electrical power separately, which requires more space for two separate machines [5]. However, it is possible to convert the input energy into mechanical and electrical power independently, using a single machine in the EAD system [1], [3], [4] making it more compact. For these EAD systems, the researchers have adapted different configurations of electrical machines.

Permanent magnet synchronous machines (PMSM) to meet the requirements of traction systems and accessory drive systems in HEV applications have been extensively researched owing to the benefits of high torque density

The associate editor coordinating the review of this manuscript and approving it for publication was Jinquan Xu.

This work is licensed under a Creative Commons Attribution-NonCommercial-NoDerivatives 4.0 License.
For more information, see https://creativecommons.org/licenses/by-nc-nd/4.0/

and compactness. For traction part, traction machines are specially designed to produce variable speed and torque requirements. For the EAD system having a separate motor and a generator, PMSM machines have wide choices of design and control. The motor is particularly designed to meet the requirements of all the mechanical loads, and the generator is designed to provide a stable output at a given torque input [6]. When it comes to the usage of a single machine providing both motor and generator operation in the EAD system, the design choices are limited, and the control becomes difficult to meet the load requirements. The control of these machines to provide both mechanical and electrical power to the respective loads relies on the configuration of its winding. Thus, the windings of these machines are designed to minimize the mutual magnetic coupling effect between the motor and generator windings to get their independent operation [7].

The dual three-phase electrical machines having two sets of overlapped windings are studied in [8]. The overlapping nature of winding exhibits a higher mutual coupling effect making it a poor choice for the independent operation of motor and generator. For such operations, the dual winding PM machines using a specific arrangement of non-overlapped nature have been studied in [9], [10], [11], and [12]. This type of winding benefits the shorter end windings, high slot fill factor, and flexible control to improve the performance [13]. Furthermore, different sets of non-overlap winding provide reliable operation of the machine as the loss of one winding set will not lead to the failure of the whole system, and the operation will be sustained at reduced power. In these machines, single-layer and double-layer winding configurations were compared for mutual coupling effect. A single-layer concentrated winding machine was suggested for low mutual coupling between the phase winding as only one coil side is accommodated in one slot [14]. However, in the single-layer winding machines, adding more coils would require many slots making the teeth weaker leading to the risk of saturation. The conventional double-layer winding machines were presented as poor candidates for independent operation and control due to higher mutual coupling between the phase winding since each slot contains two coil sides. Whereas double-layer winding provides the benefits of low harmonic content in EMF, low torque ripples, and lower losses [15]. An attempt has been made with non-overlapped double-layer winding in a modular three-phase machine to provide a smaller mutual inductance [16]. However, this machine has significant saturations in the teeth and was not studied for simultaneous operations of a motor and generator. The existing mutual coupling effect between the two sets of windings is sufficient to malfunction the independent operations required in EAD systems. Therefore, there is a need to design such a machine with a double-layer winding that provides almost zero coupling between motor and generator windings to maintain independent operation in EAD systems for HEV applications.

In this paper, a unique design of a dual-winding PMSM machine based on special slots and pole combinations, and having a double-layer concentrated configuration has been proposed for the EAD system. One set of winding is used as motor winding, and the other set of winding is used as generator winding. The independent control of these two sets of winding in the proposed machine is obtained while providing the mechanical power from the motor winding, and the electrical power from the generator winding to the respective accessory loads at the same time. For this purpose, the windings are designed to achieve a zero mutual coupling between motor and generator windings using unwound tooth providing isolation. This coupling effect has been analyzed through mutual inductances, flux linkages, induced voltages, and torque production using finite element analysis.

This paper has been divided into several sections. Section-I gives the introduction part. Section-II gives the overview of the accessory drive system. Section-III gives the motor topologies, the design concept, and the working principle of the proposed machine with an overview of the electrical accessory drive system. Section-IV presents the configuration of windings and their inductances. Section-V gives an analysis of electromagnetic performance and mutual coupling effect with different methods. Finally, the conclusion is given in Section-VI.

II. OVERVIEW OF THE ACCESSORY DRIVE SYSTEM

In conventional hybrid electric vehicles, some of the indispensable accessory loads such as the power steering pump, air conditioner compressor, heating system, lighting, and power windows need continuous power regardless of vehicle motion. This power is provided either directly from the internal combustion engine via the belt mechanism or via the Lundell alternator of an EAD system. However, a single PMSM machine (having a double-layer winding) is being proposed in the EAD system to perform multitasking while eliminating both the separate alternator and the need for engine operation when the vehicle is not moving. This EAD system is shown in Fig. 1 which offers the benefits of cost, and space utilization for installation. The motor part of the dual-winding single PMSM machine will drive the mechanical loads, and the generator part will operate the electrical loads and charge the low-voltage battery via a converter. Further, the topology of this proposed machine along with the reference machine for fair comparison is provided in the next section.

III. MACHINE TOPOLOGIES, WORKING PRINCIPLE, AND DESIGN CONCEPT

A. MACHINE TOPOLOGIES

The topologies of the reference and the proposed PMSM machines are given in Fig. 2. The reference machine contains 48 slots on the stator and 64 magnet poles on the rotor, while the proposed machine comprises of 60 slots on the stator and 64 magnet poles on the rotor. In both machines, two sets of double-layer concentrated winding (one set as M-winding for

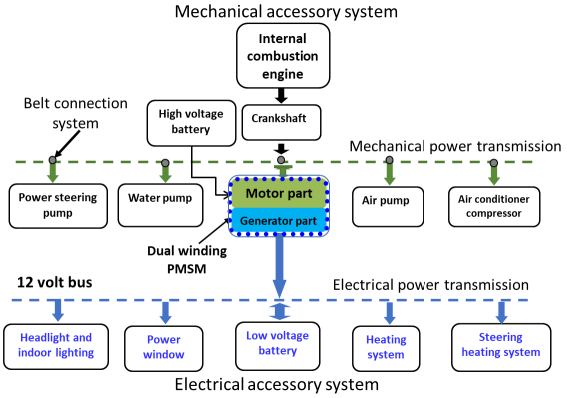

FIGURE 1. Overview of the accessory drive system with a dual-winding single PMSM machine.

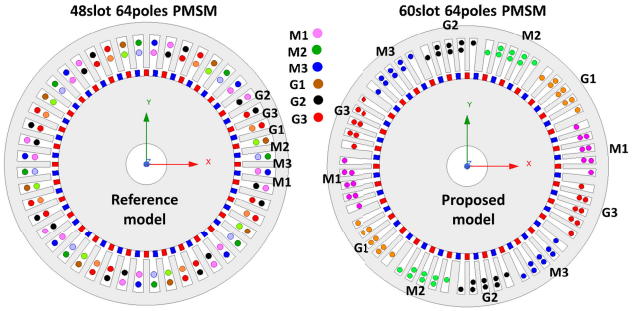

FIGURE 2. Topologies of three-phase dual-winding PMSM machines, (a) reference machine, (b) proposed machine.

the motor and another set as G-winding for the generator) are incorporated into the stator slots to accommodate 48 coils, however, the design of the proposed machine is unique in nature. In the reference machine, the winding configuration is of a typical nature with a coil span of one slot, where M1, M2, M3, G1, G2, and G3 are phases of M-winding and G-winding, respectively, as shown in Fig. 2(a). Whereas in the proposed machine, there are twelve groups of coils (having a coil span of one slot) with four coils per group on the stator. Further, these groups of coils are divided into two sets of different winding, named motor or M-winding, and generator or G-winding. Moreover, one tooth between the adjacent groups is kept unwound while maintaining the balanced three-phase winding as shown in Fig. 2(b). This makes a difference in the spatial distribution of windings in two machines. The proposed topology provides the benefits of zero mutual coupling effect between M-winding and G-winding, ease of winding, and the machine's stator can be segmented into equal parts from the tooth center of the unwound tooth for transportation convenience.

B. WORKING PRINCIPLE

In a reference PMSM machine, the coil sides of M-winding and G-winding are being overlapped in few slots due to typical nature of winding. However, in the proposed machine, the end coils of groups of M-winding and G-winding are placed in different slots separated by an unwound tooth. The

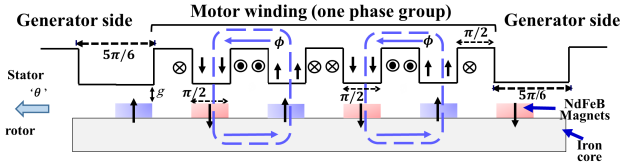

FIGURE 3. Working principle of the proposed machine showing one phase group of only M-winding.

layout of one phase group of M-winding demonstrating the working principle with the help of flux path is shown in Fig. 3. The flux from the north magnet pole enters the tooth on the stator via airgap and then returns to the adjacent south magnet pole through the stator yoke, adjacent tooth, and airgap. In the end, flux completes the loop through the rotor core. The flux linkage is experienced by both sets of winding on the stator which gives their induced back-EMF. Depending on the polarity of currents in the coils within this phase group, four rotor magnet poles are attracted and aligned with the corresponding teeth on the stator. Thus, at any instant a total of eight rotor poles are aligned with the teeth of two groups per winding phase, and the rotor continues to rotate with the excitation in the winding.

C. DESIGN CONCEPT

The proposed PMSM machine is designed such that there is zero mutual coupling between two sets of winding. To eliminate the coupling, the winding of the machine should have electrical and magnetic isolation. To achieve this isolation, the selection of slots and poles is given by (1) and (2)

$$Slots : S = m^* n_w^* n_s^* n_g \tag{1}$$

$$Poles : 2p = m^* n_w^* n_s^* n_g + 2^* n_g$$

$$n_w \geq 2, n_g \geq 2 \tag{2}$$

where 'S' is the number of slots, 'p' is the number of pole pairs on the rotor, 'm' is the number of phases, 'n_w' is the number of winding sets, 'n_s' is the number of slots for one phase group, 'n_g' is the number of groups per phase of each winding. In this paper, for $m = 3$, $n_w = 2$, $n_s = 5$, 60 slots are obtained from (1), however, for $n_g = 2$, 64 rotor poles are obtained from (2). Two sets of winding (M-winding and G-winding) have been incorporated into sixty slots such that a total of 48 coils are wound while separating each phase group of each winding by an unwound tooth. Thus, twelve unwound teeth isolate the twelve groups of these two sets of winding, six groups from each set of winding.

As the design of the proposed PMSM machine is unique in its nature. For sixty slots on the stator and sixty-four poles on the rotor, the width of all the teeth, and slots within one phase group are equal to $\pi/2$ electrical radians, whereas the width of unwound tooth separating the phase groups is equal to $5\pi/6$ electrical radians as shown in Fig. 4 to produce the symmetry in the back-EMF.

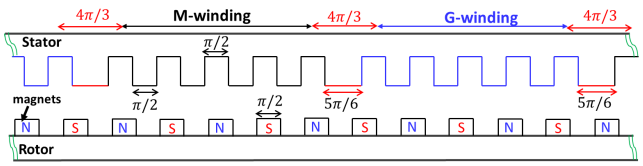

FIGURE 4. Design concept of the proposed machine showing two phase groups from both windings.

TABLE 1. Design specifications of machines.

Metrics		Reference machine	Proposed machine
Machine power, [kW]		4.5	4.5
Speed, [rpm]		1500	1500
Slots/poles		48/64	60/64
Stator outer diameter, [mm]		205	205
Stack length, [mm]		120	120
Rotor outer diameter, [mm]		128.8	128.8
Airgap diameter, [mm]		136.8	136.8
Airgap length, [mm]		1	1
No. of turns per phase for M-winding		240	240
No. of turns per phase for G-winding		120	120
Phase inductances for M-winding, [mH]		7.45	18.66
Phase inductances for G-winding, [mH]		1.86	4.66
Phase resistance for M-winding, [Ω]		1.34	1.35
Phase resistance for G-winding, [Ω]		0.67	0.675
Thickness of magnet, [mm]		4	4
Magnet	B_r, [T]	1.23	
	H_c, [kA/m]	890	

The main dimensions of the above-mentioned machines are given in Table 1.

IV. WINDING CONFIGURATION, AND MUTUAL COUPLING EFFECT

A. WINDING CONFIGURATIONS

In the reference machine, 24 coils are wound for M-winding, eight coils per phase distributed throughout the stator circumference, and the same layout of 24 coils is decorated for G-winding. Whereas in the proposed motor, the winding is a full-pitch double-layer concentrated type having coil pitch equal to the pole pitch. Six groups are formed by the 24 coils for each set of winding, two groups per phase containing eight coils such that four coils of each group are wound around the adjacent four teeth. From the topology it is clear that the slots nearest to the unwound tooth are kept partially filled to isolate the coils of each phase group. Further, the star of slot and winding function are necessary for a better understanding of winding configuration for the proposed machine.

1) STAR OF SLOT

The star of slot describes the information about winding and the phasors of induced electromotive force (EMF) [12], [16]. To find the phasors of EMF associated with each coil in the given slots, the periodicity 't' of the proposed machine is determined by the greatest common divisor (GCD) between the number of slots 'S' and the number of pole pairs 'p' given by (3)

$$t = GCD\{S,p\} = GCD\{60,32\} = 4 \tag{3}$$

The star of slot is characterized by the number of spokes. For $N_c = 48$ coils in the proposed machine, there are $N_c/t = 12$ spokes, each spoke containing $t = 4$ phasors. Now the mechanical angle between two adjacent spokes is θ_{spoke} and the electrical angle between the phasors of adjacent slots θ_{se} are given by (4)

$$\theta_{spoke} = 2\pi/(N_c/t) = \pi/6 \; radians, \theta_{se} = p^{*}\theta_{sm} = \pi \, radians \tag{4}$$

where θ_{sm} is the mechanical angle of the slot. The obtained star of slot is shown in Fig. 5. The phasors of all the coils are shown in Fig. 5 (a), where two groups containing coils 1 to 4 and 5 to 8 are associated with the first phase of M-winding. Similarly, for other phases of both sets of winding, two groups containing eight coils are associated. The spokes are shown in Fig. 5(b), where each spoke containing four phasors according to periodicity is displaced by $\pi/6$ mechanical radians. Using opposite sectors on the spokes, two sets of four phasors of two spokes associated with M1-winding are combined to form one phase as shown in Fig. 5(c). Thus, the resultant M-winding and G-winding are displaced by an angle of $(4\pi/3)-\pi = \pi/3$ electrical radians, and phases of the same winding are displaced by an angle of $2\pi/3$ electrical radians.

2) WINDING FUNCTION

The rotating MMF of stator windings has been plotted in Fig. 6 using the winding function theory [17], [18] which will help to compute their inductances. Considering the spatial distribution of the coils along the stator circumference, each coil out of four coils from one group of M-winding spans π electrical radians such that the other four coils of the second group of this winding lie in the same position as the first four coils. Whereas the first coil of one group of one phase from G-winding is after unwound tooth giving a total angle of $4\pi/3$ electrical radians. In the same pattern, MMF of other phases of M- and G-winding can be plotted at $2\pi/3$ electrical radians displaced from the first phase. Based on the plotted winding functions, the inductances will be calculated further.

B. INDUCTANCES AND MUTUAL COUPLING EFFECT

In general, a double-layer winding configuration exhibits higher mutual inductances compared to a single-layer winding [16]. However, for the proposed machine having a double-layer winding, self and mutual inductances have been studied to analyze the coupling effect between M-winding and G-winding. These inductances are given by (5) and (6) using the winding function discussed above

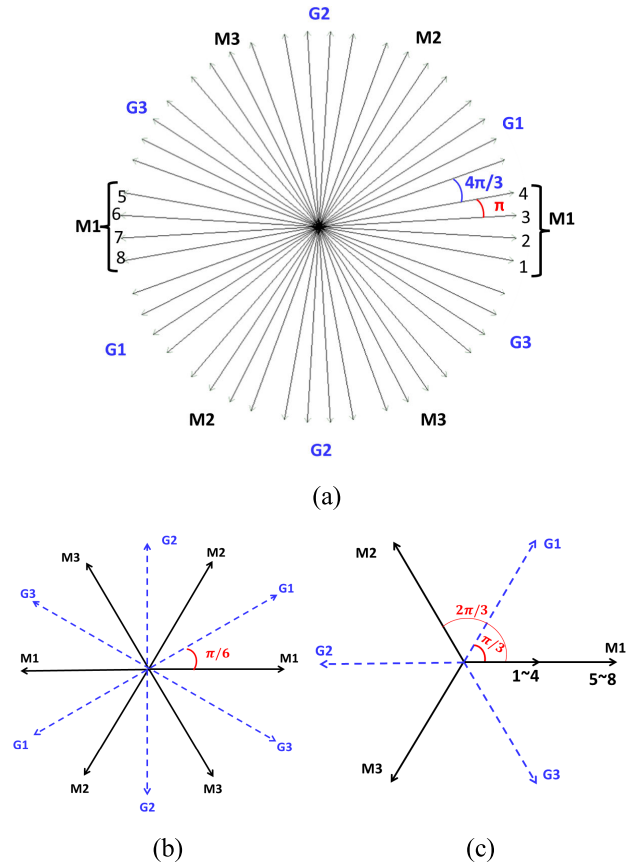

FIGURE 5. Star of slot of the proposed machine showing both M-winding and G-winding (a) all phasors of all coils with $\theta_{se} = \pi$ radians (b) spokes displaced by $\pi/6$ mechanical radians, (c) two sets of the phase winding displaced by $\pi/3$ electrical radians.

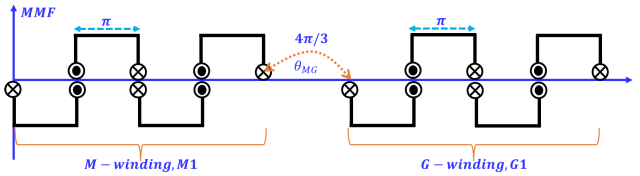

FIGURE 6. The winding function of the proposed machine showing one group of both M-winding and G-winding.

Self-inductances:

$$L_{M11} = 2^*(\mu_0 r_g l_{eff}/g)\int_0^{\pi} N_M^2(\theta)d\theta = 2\pi^*(\mu_0 r_g l_{eff}/g)N_M^2$$
$$L_{G11} = 2^*(\mu_0 r_g l_{eff}/g)\int_0^{\pi} N_G^2(\theta)d\theta = 2\pi*(\mu_0 r_g l_{eff}/g)N_G^2 \quad (5)$$

Mutual inductances:

$$L_{MG} = 2^*(\mu_0 r_g l_{eff}/g)\int_0^{\pi} N_M(\theta)^* N_G(\theta)d\theta = 0 \quad (6)$$

where L_{M11} and L_{G11} are the self-inductances of any phase of M-winding and G-winding, respectively, L_{MG} is the mutual inductance between the phases of M-winding and G-winding, μ_0 is the permeability of air, r_g is the airgap radius, g is the length of airgap, l_{eff} is the effective length of the machine, θ is the angle in radians, N_M and N_G are the turns of the M-winding and G-winding, respectively.

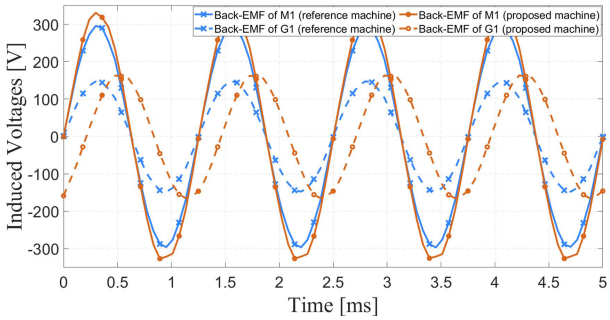

FIGURE 7. Comparison of no-load back-EMF for both machines.

From (6), it can be noted that the mutual inductances L_{MG} =0 because of the unwound teeth that provides isolation for the flux in the normal teeth of different groups and the non-overlapping nature of two sets of winding using the winding function concept. Thus, zero mutual inductance will justify the zero coupling between the M-and G-windings even using a double-layer winding type. That means the operation of M-winding will not be affected by the operation of G-winding at any time.

V. PERFORMANCE ANALYSIS

Performance characteristics for both the reference model and the proposed model are analyzed using ANSYS MAXWELL under the same operating conditions. The mutual coupling effect is characterized based on the inductances, flux linkages, and induced voltages. In addition, the output torque is compared while driving the proposed machine in different operating modes.

A. NO-LOAD BACK-EMF

The back-EMF of both motors is compared at no-load and given in Fig. 7. Having an equal number of coils, and turns per phase of each coil, the back-EMF is higher in the proposed machine than that of the reference machine. The back-EMF of M-winding is higher than that of G-winding due to the different number of turns per phase in these windings. These no-load back-EMFs will be studied for further analysis and comparing the performance between two machines for given objective.

B. MUTUAL COUPLING EFFECT ANALYSIS

To confirm the independent operation of two sets of windings, the mutual coupling effect has been investigated using different methods: 1) analysis through inductances, 2) flux linkage in one winding set having no excitation, while the other winding set is energized, and 3) analysis through back-EMF.

1) ANALYSIS THROUGH INDUCTANCES

The self and mutual inductances for each phase of each winding set are analyzed to confirm the coupling effect. First, the self-inductances of each phase of the same winding (L_{M11} and L_{G11}) for both the reference and the proposed machine

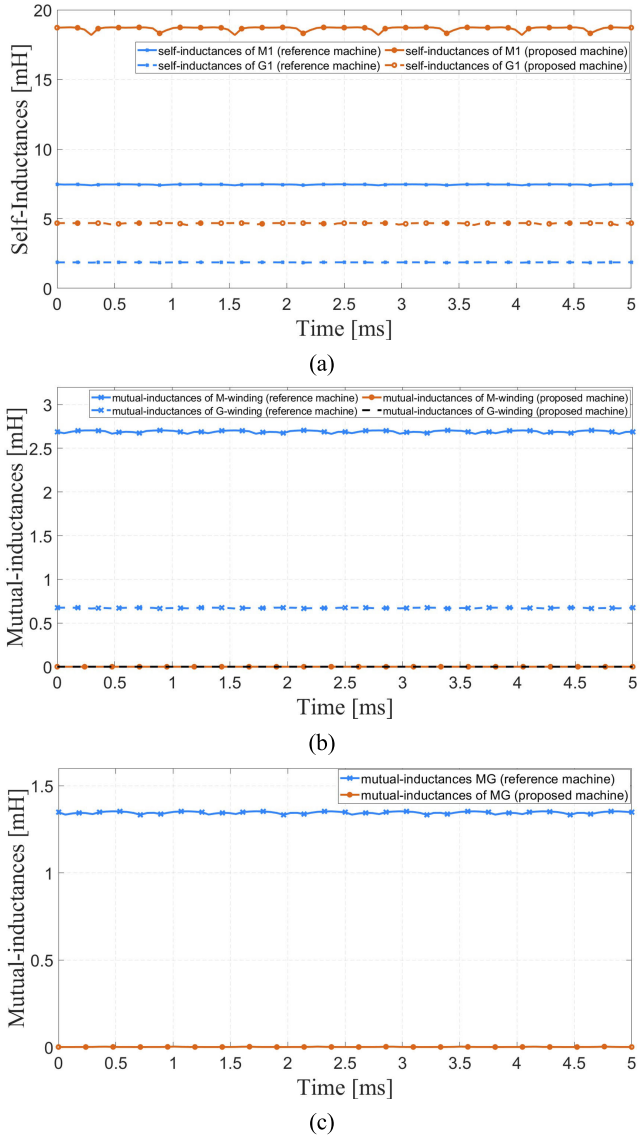

FIGURE 8. Inductances comparison of reference and proposed machines, (a) self-inductance of both sets of winding, (b) mutual inductances between phases of the same set of winding, (c) mutual inductances between the phases of M-winding and G-winding.

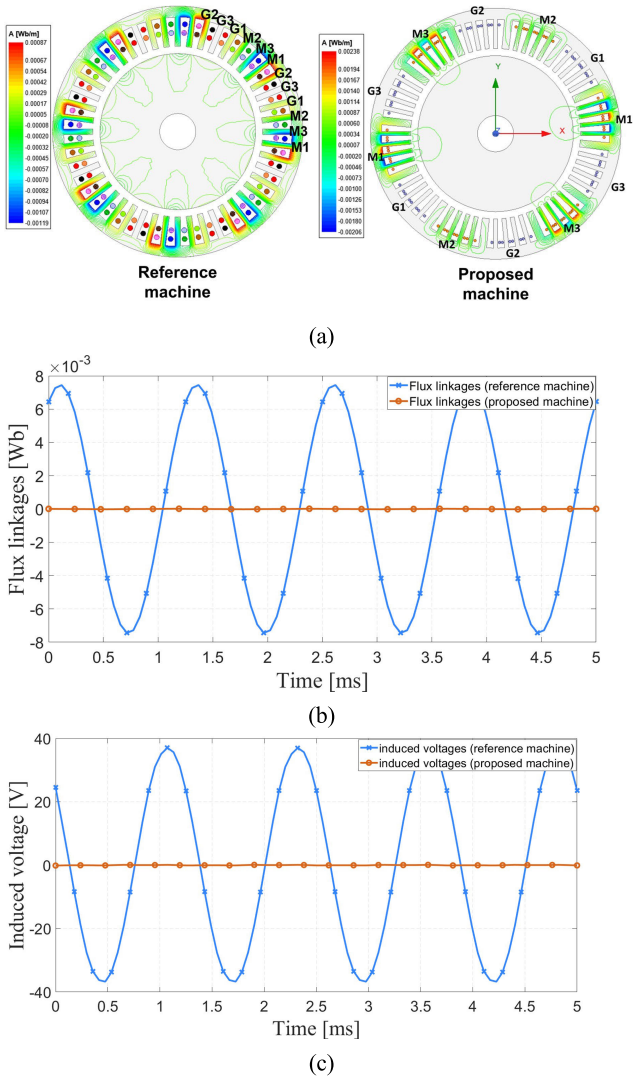

FIGURE 9. Comparison of flux distribution and induced voltages of reference and proposed machines without magnets, (a) flux lines distribution, (b) flux linkages, (c) induced voltages.

are given in Fig. 8(a), whereas the mutual inductances between adjacent phases of the same set of winding (L_{M13} or L_{G13} for the reference machine, and L_{M12} or L_{G12} for the proposed machine) are shown in Fig. 8(b). Second, the mutual inductances (L_{MG}) between the nearby phases of M-winding and G-winding (between M_1 and G_2 or M_2 and G_1 for the reference machine, and between M_1 and G_1 or M_2 and G_2 for the proposed machine) are given in Fig. 8(c). The results show the values of mutual inductances for the reference machine indicating the existence of the mutual coupling between the two sets of winding. However, these mutual inductances are zero for the proposed machine indicating zero coupling between M-winding and G-winding. Thus, the absence of the mutual coupling effect would support the independent operation of M-winding and G-winding in the proposed machine compared to that in the reference machine.

2) ANALYSIS THROUGH FLUX LINKAGES AND INDUCED VOLTAGES WITHOUT PM

In this method, the mutual coupling effect has been analyzed without a permanent magnet source on the rotor while input current is injected into M-winding, and the flux linkage or induced voltages are observed in the G-winding having no excitation. For both machines, the flux lines are shown in Fig. 9(a), which shows that several lines are routing through the teeth of G-winding indicating mutual coupling in the reference machine. Whereas, in the proposed machine, flux lines are only routed into the teeth associated with M-winding and no flux line is channeled into the teeth associated with G-winding. This signifies the isolation of two sets of winding for the proposed machine.

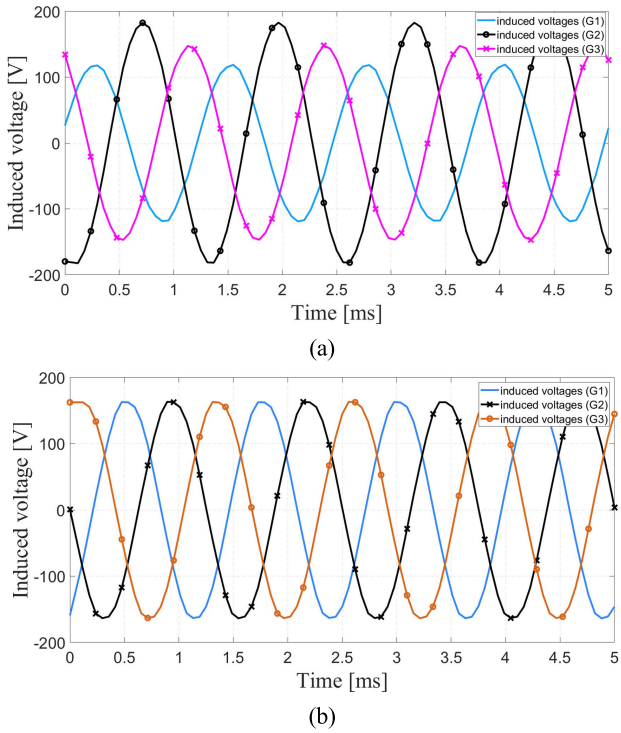

FIGURE 10. Comparison of back-EMF in G-winding when only M-winding is excited, (a) for the reference model, (b) for the proposed model.

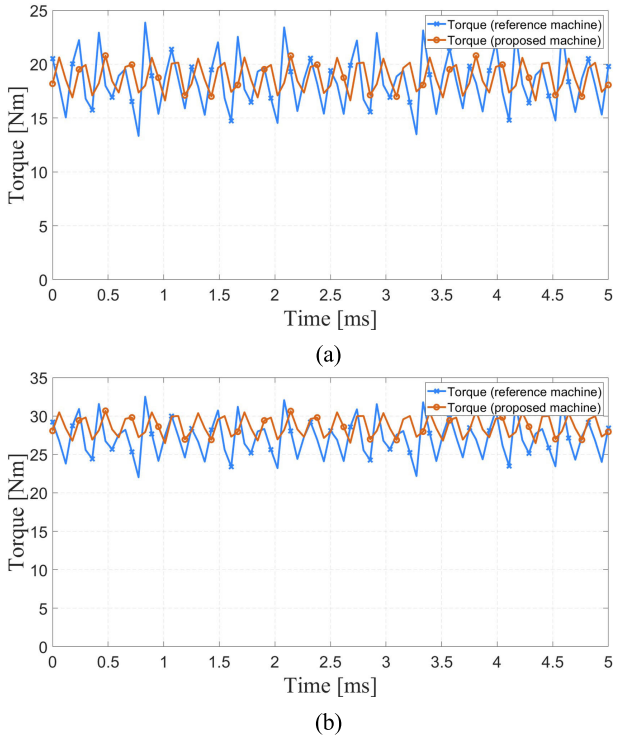

FIGURE 11. Comparison of torques for both machines, (a) when only M-winding is excited, (b) when both windings are fed by the input current (motor-motor mode).

Alternatively, flux linkage is seen in G-winding when M-winding is excited, hence the voltages are induced in G-winding in the reference machine as shown in Fig. 9(b) and Fig. 9(c). However, flux linkages, as well as induced voltages, are zero in the G-winding of the proposed machine, confirming the feasibility of the effective independent operation of two sets of windings.

3) ANALYZING THROUGH THE BACK-EMF

Now, M- winding is kept energized and the quality of back-EMF in G-winding is observed while the permanent magnets on the rotor are acting as a source of magnetic flux. The results for both the reference model and the proposed model are shown in Fig. 10. It is revealed that back-EMF in G-winding in the reference model becomes unbalanced and the root means square (RMS) value of each phase is different as shown in Fig. 10(a). This occurred due to the mutual coupling between the coil's sides of the M-winding and G-winding wound in the same slot. However, in the proposed model the back-EMF in G-winding is balanced, and the RMS values of each phase are the same showing no mutual coupling, as shown in Fig. 10(b). The same is true when back-EMF in M-winding is observed while G-winding carries the current. Thus, this analysis also proves the decoupled sets of winding in the proposed machine.

C. OPERATING MODES

Three operating modes of both machines are discussed in this section: (i) the M-winding will be energized, and the effect will be analyzed on open-circuited G-winding, (ii) load will be varied on G-winding and the effect will be analyzed on open-circuited M-winding, (iii) simultaneous operation of M-winding and G-winding.

1) MOTOR-ONLY MODE

In this operating mode, the machine is operated as a motor with the injection of current only into M-winding to produce the torque to run the mechanical loads. The G-winding is kept unenergized and no electrical load is connected at the terminals. Thus, one of the two sets of winding is being utilized this time according to the power demand depending upon the type of accessory loads. The results are depicted in Fig. 11(a), which gives a slightly greater torque value for the proposed machine compared to the reference machine under the constraints of the same electrical and magnetic loadings.

There is also a possibility of energizing both sets of winding in motor-motor mode. In this operation, the motoring power will be enhanced when there is such demand. The motoring torques are compared in Fig. 11(b) for both machines. During the motoring mode, the back-EMF of G-winding will be the same as discussed in the previous subsection (Fig. 7).

2) GENERATOR-ONLY MODE

When the shaft of the dual-winding machine is rotated with the help of an engine in the hybrid electric vehicle, the generated electricity will be utilized by the electrical loads.

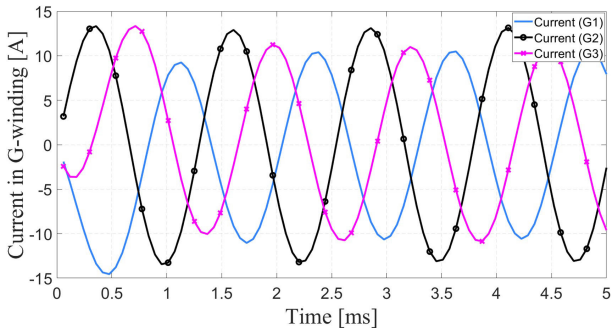

(a)

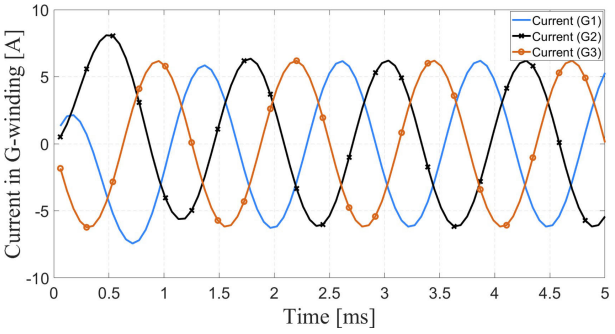

(b)

FIGURE 12. Comparison of currents in G-winding when the electrical load is connected, (a) for the reference model, (b) for the proposed model.

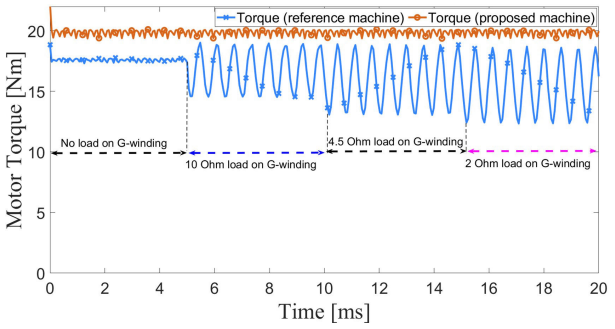

FIGURE 13. Comparison of motor torques with the variation of loads on the generator.

At this time, M-winding is open-circuited, and no mechanical load is being driven by the motor. In this case, the generated torque will be negative. The current drawn by the electrical load from G-winding for each model is shown in Fig. 12. For the reference model, currents are unbalanced as shown in Fig. 12(a), whereas, for the proposed model, the currents are balanced as shown in Fig. 12(b).

3) MOTOR-GENERATOR SIMULTANEOUS OPERATION MODE

Both sets of winding are playing their role simultaneously in this operating mode. Motoring power is utilized to drive the mechanical loads, whereas generator power is utilized to run the electrical loads. The motoring torque is obtained with the varying electrical load on the G-winding side as shown in Fig. 13. In this case, the waveforms of induced voltages

TABLE 2. Performance comparison at no-load operation.

No-load Operation			
Metrics		Reference machine	Proposed machine
Inductances, [mH]	L_{M11},	7.45	18.66
	L_{G11}	1.86	4.66
	L_{M1M3},	2.69	0.0000
	L_{G1G3}	0.67	0.0000
	L_{M1G1}	1.35	0.0017
Flux linkages, [Wb]	M-winding	0.0416	0.0470
	G-winding	0.0208	0.0235
Back-EMF, [V]	M-winding	208.4	235.4
	G-winding	104.2	117.8

TABLE 3. Analysis of mutual coupling effect without magnets.

M-Winding is excited, and the rotor is without PM			
Metrics		Reference machine	Proposed machine
Flux linkages, [Wb]	G-winding	0.0053	0.0000
Back-EMF, [V]	G-winding	26.4	0.05

in M-winding were observed and stored. These waveforms of individual phases are multiplied by their corresponding input currents. The results are added together and divided by synchronous speed 'ω' to find out the resultant torque as given by (7).

$$T = (1/\omega)^*(E^*_{m1}I_{m1} + E^*_{m2}I_{m2} + E_{m3}{}^*I_{m3}) \tag{7}$$

where E_{m1}, E_{m2}, E_{m3} are back-EMFs of different phases of M-winding, and I_{m1}, I_{m2}, I_{m3} are input currents to these phases of M-winding.

It can be seen that the average value of motor torque for the proposed model is unchanged with the variation in load on the generator side due to the elimination of the coupling effect, whereas the average torque for the reference model decreases accompanied by high torque ripples. This occurs due to the mutual coupling effect in the reference model.

D. RESULTS AND DISCUSSIONS

The performances of both the reference and the proposed machines are compared based on the coupling effect of M-winding and G-winding, and their operations under the same design constraints. The results of inductances, flux linkages, and EMF of M-winding and G-winding at no-load conditions are given in Table 2. The self-inductances are improved, and the mutual inductances between the different phases of the same winding and between the phases of M-winding and G-winding are zero indicating the superiority of the proposed machine in terms of magnetic decoupling. In addition, the flux linkage and the EMF of M-winding and G-winding in the proposed machine are improved compared to those of the reference machine.

TABLE 4. Analysis of mutual coupling effect with magnets.

M-Winding is excited, and the rotor is with PM			
Metrics		Reference machine	Proposed machine
Flux linkages, [Wb]	G-winding	0.0168,0.0258, 0.0207	0.0235
Back-EMF, [V]	G-winding	84,129,104	117.7, 117.7, 117.7
Result type	-	Unbalanced	Balanced

TABLE 5. Performance comparison at only-motor operation.

Motor-only Operation			
Metrics		Reference machine	Proposed machine
Motor Torque, [Nm]	Using M-winding only	18.35	18.8
	Motor-motor mode	27	28.7
Input current, [A_{rms}]	-	4.4	4.4

TABLE 6. Performance comparison at only-generator operation.

Generator-only Operation			
Metrics		Reference machine	Proposed machine
Flux linkages, [Wb]	M-winding	0.039,0.033, 0.042	0.0470
Back-EMF, [V]	M-winding	196, 168, 209	235.4
Result type	-	Unbalanced	Balanced

The results of the analysis of the mutual coupling effect based on flux linkage and induced voltages are given in Table 3 and Table 4. Without magnets on the rotor, both the flux linkages and induced voltages in the G-winding of the proposed motor are negligible compared to that in the reference motor. These results indicate that there is no mutual coupling between the M-winding and G-winding of the proposed motor. Likewise, with the magnets on the rotor, flux linkages and induced voltages in the G-winding of the reference motor are unbalanced exhibiting a mutual coupling effect, however, induced voltages remain unchanged as well as balanced in the case of the proposed machine indicating no mutual effect of two sets of windings.

Furthermore, the individual operation of each winding is analyzed as only-motor and only-generator operations. For only-motor operation, motor torques are compared in Table 5. For only-generator operation, induced voltages in M-winding are observed and given in Table 6. Again, these voltages are unbalanced due to a mutual coupling effect similar to the results in Table 4.

TABLE 7. Performance comparison at simultaneous operation.

Motor and Generator Simultaneous Operation			
Metrics		Reference machine	Proposed machine
Motor Torque	with varying load on generator	Decreases	Remains unchanged
Torque ripples		Increases	Remains unchanged

Finally, the simultaneous operation is performed while injecting the current into the M-windings and varying the load on the generator terminals and compared in Table 7. The motor torque decreases, ripples increase, and unbalanced currents flow in the case of the reference machine, whereas torque and ripples remain unchanged for the proposed machine. This confirms the independence of the two sets of windings in the proposed machine for the accessory drive system in hybrid electric vehicles.

In addition, the efficiencies of both machines were calculated by considering their copper and core losses considering the same operating mode at input RMS current of 4.4 A. The total losses for the reference and proposed machines are 344 W (core losses 305 W, copper losses 39.14 W) and 414 W (core losses 374.8, copper losses 39.14 W), respectively. These losses are larger in the proposed machine due to increased core losses because of higher flux density in the teeth of the particularly designed stator. The resulting efficiencies of these machines are 91.9 % and 90.8%, respectively. The efficiency is significantly lower in the proposed machines than that of the reference machine due to increased losses.

VI. CONCLUSION

A single PMSM machine providing multitasking is proposed in this paper. For this purpose, a PMSM machine having special slots and pole combinations with double-layer concentrated configuration of winding was designed forming two sets of windings separated by the unwound tooth between the phase groups on the same stator. The unwound teeth help in providing an isolation to achieve the independent operation of motor and generator winding, which is verified by analyzing the mutual coupling effect. The analysis results confirm zero mutual coupling (isolation) between M-winding and G-winding for the proposed machine, L_{MG} =0. However, the reference machine exhibits a significant mutual coupling which deteriorates the simultaneous operation of these two sets of windings. Thus, the proposed PM machine with a special structure is valuable to achieve motor and generator simultaneous operation without any interference.

AUTHOR CONTRIBUTIONS

Conceptualization, Tanveer Yazdan.; methodology, Tanveer Yazdan.; writing—original draft preparation, Tanveer Yazdan, and Muhammad Humza.; writing—review and editing,

Tanveer Yazdan, and Muhammad Humza.; Funding acquisition, Han-Wook Cho. All authors have read and agreed to the published version of the manuscript.

REFERENCES

[1] K. V. Singh, H. O. Bansal, and D. Singh, "A comprehensive review on hybrid electric vehicles: Architectures and components," *J. Mod. Transport.*, vol. 27, pp. 77–107, Jun. 2019.

[2] F. Un-Noor, S. Padmanaban, L. Mihet-Popa, M. Mollah, and E. Hossain, "A comprehensive study of key electric vehicle (EV) components, technologies, challenges, impacts, and future direction of development," *Energies*, vol. 10, no. 8, p. 1217, Aug. 2017.

[3] M. Tezcan, E. Mese, I. Ustoglu, and M. Ayaz, "Analytical modeling of dual winding surface-mounted permanent magnet synchronous machine for hybrid electric vehicle accessory drive systems," *Electr. Power Compon. Syst.*, vol. 45, no. 12, pp. 1353–1369, Jul. 2017.

[4] E. Mese, Y. Yasa, H. Akca, M. G. Aydeniz, and M. Garip, "A new electric accessory drive system for hybrid electric vehicles," in *Proc. IEEE Energy Convers. Congr. Expo. (ECCE)*, Sep. 2012, pp. 1909–1916.

[5] R. K. Serrels, "Accessory drive system," U.S. Patent 20 080 020 875, Jan. 24, 2008.

[6] T. Martin, "Hybrid vehicle transmissions and transaxles," in *Hybrid and Alternative Fuel Vehicles*. London, U.K.: Pearson, 2011.

[7] E. Mese, M. Ayaz, and M. M. Tezcan, "Design considerations of a multitasked electric machine for automotive applications," *Electr. Power Syst. Res.*, vol. 131, pp. 147–158, Feb. 2016.

[8] E. Fuchs and L. Rosenberg, "Analysis of an alternator with two displaced stator windings," *IEEE Trans. Power App. Syst.*, vol. PAS-93, no. 6, pp. 1776–1786, Nov. 1974.

[9] F. Barrero and M. J. Duran, "Recent advances in the design, modeling, and control of multiphase machines—Part I," *IEEE Trans. Ind. Electron.*, vol. 63, no. 1, pp. 449–458, Jan. 2016.

[10] M. Barcaro, N. Bianchi, and F. Magnussen, "Six-phase supply feasibility using a PM fractional-slot dual winding machine," *IEEE Trans. Ind. Appl.*, vol. 47, no. 5, pp. 2042–2050, Sep./Oct. 2011.

[11] M. Ayaz, M. Tezcan, K. Yilmaz, and E. Mese, "Magnetic coupling effect of a PM synchronous machine having concentrated windings," in *Proc. 6th IET Int. Conf. Power Electron., Mach. Drives (PEMD)*, 2012, p. 153.

[12] E. Mese, M. Ayaz, M. Tezcan, and K. Yilmaz, "Design of dual winding permanent magnet synchronous machines for hybrid electric vehicle accessory drives," *Int. J. Vehicle Des.*, vol. 69, nos. 1–4, pp. 185–207, 2015.

[13] K. S. Garner and M. J. Kamper, "Performance comparison of large-scale design-optimized non-overlap and overlap winding wound rotor synchronous generators," *IEEE Trans. Ind. Appl.*, vol. 59, no. 1, pp. 759–766, Jan. 2023.

[14] E. Mese, Y. Yasa, H. Akca, M. G. Aydeniz, and M. Garip, "Investigating operating modes and converter options of dual winding permanent magnet synchronous machines for hybrid electric vehicles," *IEEE Trans. Energy Convers.*, vol. 30, no. 1, pp. 285–295, Mar. 2015.

[15] D. Ishak, Z. Q. Zhu, and D. Howe, "Comparison of PM brushless motors, having either all teeth or alternate teeth wound," *IEEE Trans. Energy Convers.*, vol. 21, no. 1, pp. 95–103, Mar. 2006.

[16] Y. Li, Z.-Q. Zhu, X. Wu, A. S. Thomas, and Z. Wu, "Comparative study of modular dual 3-phase permanent magnet machines with overlapping/non-overlapping windings," *IEEE Trans. Ind. Appl.*, vol. 55, no. 4, pp. 3566–3576, Jul. 2019.

[17] N. Bianchi, S. Bolognani, M. D. Prè, and G. Grezzani, "Design considerations for fractional-slot winding configurations of synchronous machines," *IEEE Trans. Ind. Appl.*, vol. 42, no. 4, pp. 997–1006, Jul./Aug. 2006.

[18] T. A. Lipo, *Introduction to AC Machine Design*. Hoboken, NJ, USA: Wiley, 2017.

TANVEER YAZDAN was born in Jampur, Punjab, Pakistan. He received the bachelor's degree in electrical engineering from the University of Engineering and Technology, Taxila, Pakistan, in 2010, and the M.S. degree leading to Ph.D. degree in electrical engineering from Hanyang University, South Korea, in 2018. From 2010 to 2013, he was an Assistant Manager with Karachi-Electric Company, Pakistan. He is currently an Assistant Professor with The University of Lahore, Pakistan. His research interest includes the design and control of electrical machines.

MUHAMMAD HUMZA was born in Jampur, Punjab, Pakistan. He received the bachelor's degree in electrical engineering from FUUAST Islamabad, Pakistan, in 2012, and the M.S. degree leading to Ph.D. degree in electrical engineering from Kunsan National University, South Korea, in 2018. From December 2018 to August 2022, he was an Assistant Professor with the Institute of Southern Punjab Multan, Pakistan. Currently, he is a Postdoctoral Researcher with Chungnam National University, South Korea. His research interests include the design of electrical machines and power electronics.

HAN-WOOK CHO (Member, IEEE) received the B.S., M.S., and Ph.D. degrees from Chungnam National University, Daejeon, South Korea, in 2002, 2004, and 2007, respectively. From September 2007 to August 2010, he was a Senior Researcher with the Korea Institute of Machinery and Materials. From 2016 to 2017, he was a Visiting Scholar with the Department of Electrical and Computing Engineering, University of Illinois Urbana–Champaign, Urbana, IL, USA. He is currently a Professor with the Department of Electrical, Electronics, and Communication Engineering Education, Chungnam National University.